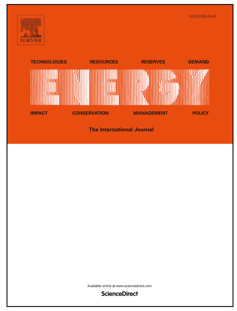

Geothermal heat exchanger energy prediction based on time series and monitoring sensors optimization

Bruno Baruque, Santiago Porras, Esteban Jove, José Luis Calvo-Rolle

PII: S0360-5442(18)32581-7

DOI: https://doi.org/10.1016/j.energy.2018.12.207

Reference: EGY 14460

To appear in: *Energy*

Received Date: 27 September 2018

Revised Date: 29 November 2018

Accepted Date: 27 December 2018

Geothermal heat exchanger energy prediction based on time series and monitoring sensors optimization

Bruno Baruque[a], Santiago Porras[b], Esteban Jove[c], José Luis Calvo-Rolle[c]

[a] *Universidad de Burgos, Departamento de Ingeniería Civil, C/ Francisco de Vitoria, s/n, 09006, Burgos, Burgos, Spain*
[b] *Universidad de Burgos, Departamento de Economía Aplicada, Plaza Infanta Doña Elena, s/n, 09001, Burgos, Burgos, Spain*
[c] *University of A Coruña, Department of Industrial Engineering, Avda. 19 de febrero s/n, 15405, Ferrol, A Coruña, Spain*

Abstract

In recent years, the use of renewable energies has been promoted in most of developed countries due to the climate change threat. In this scenario, the importance of geothermal installations has increased. This paper focuses on a heat exchanger present on a geothermal installation. The main aim is to achieve an accurate prediction system using the previous readings of some of the sensors located along the heat exchanger. Different time series modeling techniques were applied obtaining satisfactory results in the prediction of the heat exchanger state during one year. This prediction is made one hour, three hours and six hours in advance. Also, a strong correlation between the sensor readings is concluded, offering the possibility to dispense some of them.

Keywords: Time series modeling, TDNN, ARIMA, Ridge Regression, Decision Trees, MLP

Email addresses: bbaruque@ubu.es (Bruno Baruque), sporras@ubu.es (Santiago Porras), esteban.jove@udc.es (Esteban Jove), jlcalvo@udc.es (José Luis Calvo-Rolle)

1. Introduction

In last decades, the world is facing fast changes in terms of economic global instability, increase in competitiveness and climate change [1]. Under these circumstances, the rising price of raw materials and a high fossil fuels dependency, with the corresponding environment damage, led to an intensification in the use of alternative energy resources [2]. The supply of renewable energies is unlimited, and its use is relatively clean. For these reasons, during last decades, many governments have promoted policies that encourage the use of these kind of energies [3].

Usually, solar and wind are the most used alternative energies, and therefore, their technologies have experienced an intense development. However, nowadays, the field of renewable energies have presented significant advances in other disciplines such as geothermal or ocean energies [4]. These advances are aimed at narrowing the implantation costs and increasing the efficiency. Some researches are focused on developing new methods or optimizing existing ones in energy installations [5]. In some systems, different renewable energies like geothermal and solar are combined to improve the efficiency [6].

This paper focuses on a geothermal energy installation. Geothermal is defined as the energy stored in form of heat inside the earth under the ground [7]. Different works estimate that the whole amount of heat flowing from inside the earth is around 42×10^{12} W [7]. Only the 2 % of this energy comes from the crust, the 82 % comes from the mantle due to the decay of radioactive isotopes of uranium, potassium and thorium and the remaining percentage is generated at the core. Despite the vast amount of energy, its use is limited to specific areas with proper geological conditions [8].

At the beginning of twenty first century, the use of geothermal energy to produce electricity had an installed capacity of almost 9 MW, while its use in non-electrical applications represented about 15 MW. The use of non-electrical geothermal energy is extended in applications like heat pumps, bathing, space heating, green houses, aquaculture and industrial processes [7].

A heat pump is employed to provide thermal energy obtained from an external source to a facility [9]. The external source can be hot or cold, leading the first one to higher efficiency. In geothermal heat pumps, the thermal source is hot and the heat exchanger installation can be placed in horizontal or vertical configurations [10, 11]. Vertical configuration leads to a more efficient installation because at a significant depth, the ground temperature tends to remain constant along the year. This means that ground temperature is lower than air temperature in summer and is higher in winter. On the other hand, horizontal configurations are placed near the ground surface and therefore, the temperature varies significantly depending on the season of the year. However, the high cost of vertical configuration boreholes usually forces to use the horizontal configuration, whose installation turns out to be more economical [12]. With the aim of increasing the energy efficiency in the horizontal configurations, the exchanger is commonly placed deeper in the ground [13]. If a good performance is desired in the heat exchange, the accurate performance of the geothermal installation is mandatory to be known.

This work deals with a geothermal heat exchanger located on a bioclimatic house. The installation operation is recorded during one year using the temperature sensors along the exchanger.

Different works show the importance of predicting parameters like temperature soil or thermal resistance of geothermal installation [6, 14]. This paper proposes a method to model and predict the behavior of the geothermal heat exchanger using different time series techniques from the initial dataset. To do that, two different training set variations have been tested: the first one consisted of using only the previous month to predict the next one, while the second one consisted of training with all data available up to a certain point to predict the measures for the next month. Also, a comparison between modeling with all the data and only with data from cases where the heat pump is not turned off in a steady state is made.

Satisfactory results were obtained in general terms, and a good prediction of the heat exchanger is achieved one, three and six hours in advance. Also, it is concluded that there is a strong correlation between different sensors located along the installation.

This paper is structured as follows. After the present introduction, the case of study is briefly described. Then, the used techniques section is presented, followed by the experiments set up. Experiments and results are shown in next section and finally, conclusions and future work are exposed.

2. Case of study

The present research describes a novel model that is able to predict the behavior of a heat exchanger located in a geothermal installation. This installation is part of the Sotavento bioclimatic house, briefly described in the next subsection.

2.1. Sotavento bioclimatic house

The bioclimatic house under study is the result of a project developed by Sotavento Galicia Foundation, whose aim is to demonstrate the feasibility of the different renewable sources and spread their use. This house is placed in the facilities of the Sotavento Experimental Wind Farm, which is located between the councils of Monfero (A Coruña) and Xermade (Lugo), in the autonomous community of Galicia (Spain). Its geographical coordinates are 43° 21' North, 7° 52' West. It is located at a height of 640 m and is 30 km away from the sea.

Different renewable energy sources supply the thermal and electrical installation of the bioclimatic house. The electrical energy is supplied by wind generators and photovoltaic panels. Furthermore, when these sources are not enough to cover the demand, the power grid also provides electrical energy to the lighting and power systems of the house.

On the other hand, the thermal installation is in charge of the heating system and the DHW (Domestic Hot Water). For this task, solar, geothermal and biomass energies are exploited.

This installation has three main different parts: generation, consumption and accumulation:

Generation. Three energy resources supply thermal energy to the installation:

- The solar thermal system consists of eight solar panels that absorb energy from the solar radiation and uses it to heat the fluid flowing inside them. This heated fluid is driven to the heat exchanger placed in a water accumulator, where the water is stored at high temperature for later use.

- The biomass system has a boiler with configurable power, from 7 kW to 20 kW, with a yield of pellets of 90 %. This system supplies hot water directly to an inertial accumulator at 63 $^{\circ}C$.

- The geothermal system consists of a horizontal collector with five 100 meter loops. The exchanger is placed two meters under the ground. It has a nominal heating power of 8.4 kW and a nominal electrical power consumption of 1.9 kW. The warmth from the ground heats up a fluid that warms the water driven directly to the inertial accumulator.

Accumulation. The solar accumulator has a volume of 1000 liters. This accumulator is connected in series with an inertial accumulator of 800 liters. Furthermore, it receives energy from the geothermal system and the biomass boiler. The use of inertial accumulators is commonly suggested in all heating systems. Its main objective is to minimize the start-stop cycles of the unit.

Consumption. Installation of Domestic Hot Water (DHW) and underfloor heating are supplied by an inertial accumulator. The DHW supplies a bathroom and a kitchen. The system was dimensioned according to the Spanish Technical Building Code (240 liters per day). The underfloor heating system is able to keep the house temperature between 18 $°C$ and 22 $°C$. For this purpose, the water temperature remains between 35 $°C$ and 40 $°C$.

As explained in the Introduction section, this paper focuses on the geothermal installation, which is described in detail in the next subsection.

2.2. Geothermal system under study

The topology of the horizontal heat exchanger installation with the Heat Pump is shown in Figure 1. Two main different circuits are connected to the Heat Pump. The primary circuit consists of a geothermal exchanger that supplies the heat from the ground to the Heat Pump. The second circuit connects the inertial accumulator to the Heat Pump.

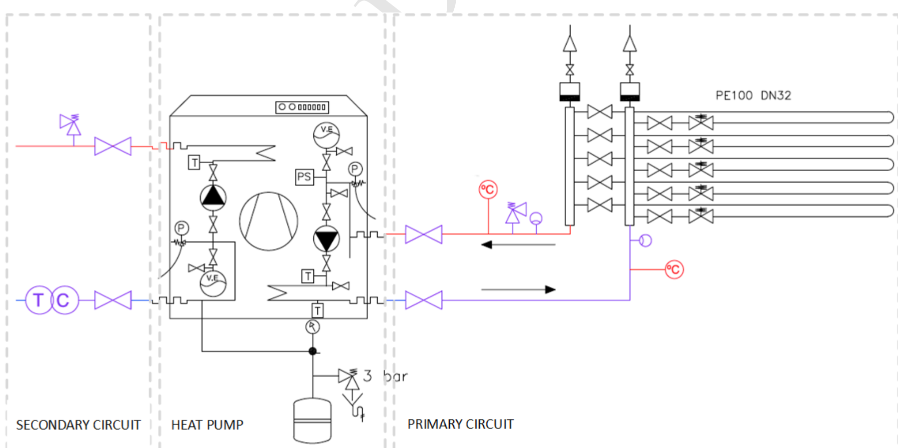

Figure 1: Geothermal installation

The geothermal exchanger has five circuits. With the aim of monitoring the ground temperature while the system is operating, different sensors are located along the heat exchanger. These sensors are distributed in four loops.

The sensors layout of one of the five circuits is shown in Figure 2, being the S401 the sensor that measures the ground temperature.

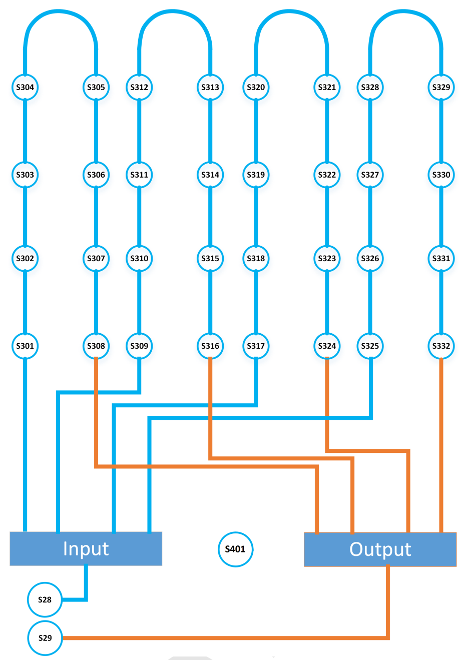

Figure 2: Geothermal exchanger sensors layout

2.3. Dataset obtaining and description

The set of temperatures measured at the geothermal heat exchanger were recorded during one year. The measures consisted of 29 features that were registered with a 10 minutes sample rate. With the aim of avoiding wrong performance of the model, a preliminary inspection of the dataset was carried out. It is found that three measurements in one day of the year are duplicated. These values are considered not valid, so after discarding them, the 52.645 initial samples were reduced to 52.639.

3. Regression Models Description

In this section we are summarizing the techniques used to predict the heat exchanger pump behavior and perform a comparative study among all of them.

3.1. ARIMA

A classical model for time analysis is ARIMA (autoregressive integrated moving average) proposed by Box and Jenkins in 1970, with a more recent review published in [15]. This is a quite well-known technique for time series analysis. The model has been widely used in economy, especially in stock markets forecasting, chain supply problems, prediction of electricity prices, etc. Also, it has been used in temperature analysis and natural phenomena prediction [16, 17], among others.

ARIMA process is composed of three phases: a preliminary stage of data preparation, a subsequent parameter estimation and model selection, and a final model checking and forecasting stage. Data preparation involves transformations and differencing. Data transformations (square roots or logarithms) stabilize the variance in series in which variation changes with the level. Next, the data must be differenced until there are no obvious patterns such as trend or seasonality. Parameter estimation aims to find the values of the ARIMA model coefficients which best fit to the data, while model checking involves testing the previous assumptions. Once the model has been selected, estimated and checked, it is usually a straightforward task to compute forecasts: in our case, we apply the obtained model to the test data and analyze the fitness of the prediction.

Typically an ARIMA model is denoted $ARIMA(p, d, q)$ where: p is the order of the autoregressive part, d is the order of the differencing and q is the order of the moving-average process. In our tests, we used the ARIMA (0,0,1) also known as MA(1) or moving averages and the ARIMA (0,0,0) also known as a random walk model, more used in monthly periods. Since both obtained very similar results, only the first one will be referenced in the experiments description.

3.2. Ridge Regression

Ridge Regression was proposed by Hoerl and Kennard [18]. Ridge regression addresses some of the problems of Ordinary Least Squares by imposing a penalty on the size of coefficients. When multicollinearity occurs, least squares estimates are unbiased, but their variances are large so they may be far from the true value. By adding a degree of bias to the regression estimates, ridge regression reduces the standard errors. It is hoped that the net effect will be to give estimates that are more reliable.

The ridge coefficients minimize a penalized residual sum of squares: $min_w||X_w - y||2^2 + \alpha||w||2^2$. Here, $\alpha \geq 0$ is a complexity parameter that controls the amount of shrinkage: the larger the value of α, the greater the amount of shrinkage and thus, the coefficients become more robust to collinearity. It has been used in problems related to temperature and time series [19] and in building energy consumption [20]. In our case we have used a Python implementation [21].

3.3. Decision Trees

Decision Tree is a well-known method used for both classification and regression tasks. These family of models was first introduced by Stone in his work [22].

Decision Trees have been use for weather and other atmospheric phenomenon forecasting tasks [23], also for energy consumption [24, 25]. A full description of these techniques can be found in [26].

In our case we have used a Python implementation [21], which uses a variant called CART (Classification and Regression Trees). The algorithm creates a multiway tree, finding for each node the categorical feature that will yields the largest information gain for categorical targets. The CART model supports numerical target variables, so it can be used in regression tasks. It constructs binary trees using the feature and threshold that yields the largest information gain at each node.

3.4. Multi-Layer Perceptron (MLP)

This well-known technique belongs to the supervised automated learning techniques. Also used in classification and regression tasks, was introduced in [27]. The concept of multi-layer perceptron is simple, it is a neural network conformed by several layers, three at least.

Input layer: conformed by the nodes that introduce the data into the neural network, receiving the input signals, but does not perform any process.

Hidden layers: this layers, also called intermediate layers do not have contact with the input signals, the elements have different connections and process the input data with activation functions. The result is transferred to the output layer.

Output layer: represents the output solution.

In temperature analysis MLP has been used in works like [28] and in studies related with building energy such as [29, 30]. In general terms, this technique shows successfully results in a wide variety of applications [31, 32, 33]. In our case, we have used the Python implementation found in [21].

3.5. Time delay neural networks (TDNN)

These neural networks were first introduced in [34]. The particularity of these neural networks is that they include a temporal dimension. They are part of the family of nonlinear auto-regressive neural networks. Time Delay Neural Networks architectures enable the networks to take into account data from different instants in time. They are all modeled as a feed-forward schema with only one hidden layer. In the input layer, we can select the number of step delays that can be used over the series fed to train, configuring, therefore, the training with a certain step. The middle layer filters the inputs before entering them into the output layer. The way in which the output layer is connected back to the input layer is what determines the variants of this model in the time series analysis. The TDNN works like other neural networks, which are based in multiple interconnected layers similar to those of the Perceptron, receiving information of the input layers, and transmiting it to the output layers. The main difference lies in the fact that these neural networks have a delay component. In order to analyze patterns or time-invariant structures, older activation and connection values of the input layers have to be stored. This is performed by making a copy of the previous values with all their outgoing connections in each time step, before updating the original values. TDNN has been widely used in the field of word and speech recognition. In the field of temperature or forecasting we have several examples like: [35, 36]. In addition, we can find examples in building energy consumption such as [37, 38]. In this work we have used the Matlab software [39].

A more detailed description of the variants of the TDNN schema used are presented in next subsection.

3.5.1. Non-Linear Input-Output (NIO)

It consists of a feed-forward network with a tapped delay line at the input. This is called the focused time-delay neural network (FTDNN). This is part of a general class of dynamic networks, called focused networks, in which the dynamics appear only at the input layer of a static multilayer feed-forward network. It is the simplest model and it is not one of the best performing, since it seems clear that once you get the previous states of the dynamic system these would be a valuable information to include also into the model for predicting future states. An implementation can be found in Matlab's Neural Network Toolbox, which has also been used in [36]. A scheme of NIO adapted from Matlab Neural Network ToolBox is presented in Figure 3,

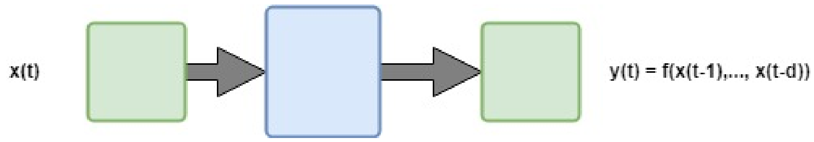

Figure 3: NIO Scheme adapted from Matlab Neural Network Toolbox.

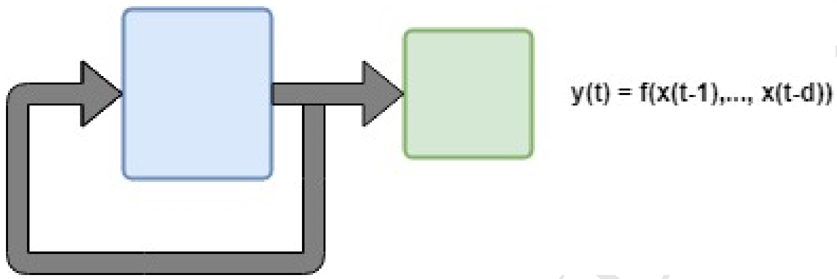

Figure 4: NAR Scheme adapted from Matlab Neural Network Toolbox

the first green square represents the input layer, the blue one the differente hidden layers and the last green square the output layer.

3.5.2. Non-Linear Autoregressive (NAR)

In this case, only the series to be approximated is used in the network training. The feed-forward network uses previous readings of the series in order to predict the new ones and additionally, includes the outputs generated in previous states as input of the following ones. This enables this architecture to maintain a certain "memory" of past states to better predict the next. In order to provide enough dimensions for the network to improve its characteristic parallel computing capabilities, the system uses a delay, which means that it will feed the network with several past steps of the series.

3.5.3. Non-Linear Autoregressive with External Input (NARX)

This model takes elements from the previous two, with the exception that in this case the network uses for its training both the previous samples of the series to be predicted and previous generated outputs of the network; along with other external attributes of the system that were sampled in the same time instant as the ones in the analyzed series. This helps the network

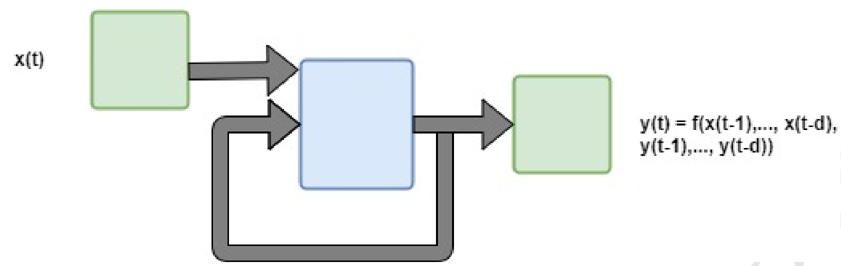

Figure 5: NARX Scheme adapted from Matlab Neural Network Toolbox

to incorporate data that is not directly correlated with the modeled system, but can have a clear influence on it. A more detailed explanation of NARX can be found in [40] and more recently in [41].

NAR and NARX have been widely used in literature, much more than NIO and it has been demonstrated that achieve better results like in [41, 42, 43, 38].

4. Experimental Set up

The real case of study used for testing consists of temperature readings for each of the sensors distributed along the described circuit plus the ground temperature sensor. Readings were taken along a complete year (2012), with a time frequency of the readings of 10 minutes. Therefore, the total amount of data samples included 52.645 samples of 29 features. Few of them had clearly identifiable errors and were discarded, so the final dataset had 52.639 samples.

An exploratory analysis of data was performed as an initial state of the work. The readings of the sensors were first compared with a statistical Pearson correlation coefficient to assess the correlation between measures: as expected by the configuration of the heat pump and the sensors, S28 and S29 where very highly correlated (0.99) as were S30 and S31 among them (also 0.99). Both pairs of sensors were inversely correlated: S28 and S29 with S30 and S31 (-0.76 to -0.82), being one pair the input and one pair the output of the heat pump. The rest of the sensors were also highly correlated among them, being all sensors included in the same connected circuit.

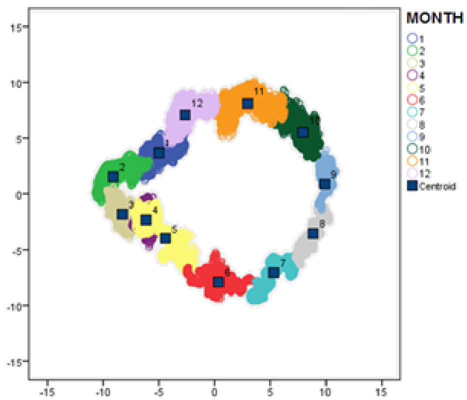

(a) Cluster distribution obtained from LDA with the complete dataset (separated by months)

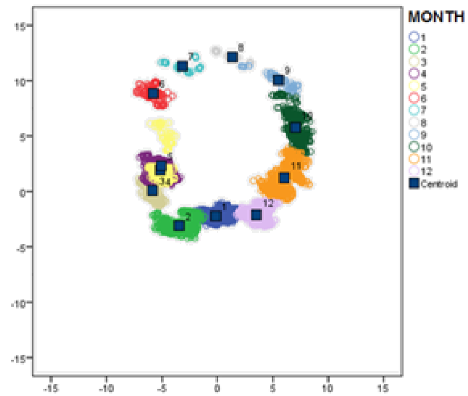

(b) Cluster distribution obtained from LDA with only the samples when the pump is working (separated by months)

Figure 6: Cluster distribution obtained from LDA

Therefore, the remaining efforts were focused on studying the prediction of the readings in a particular sensor in order to anticipate the state of the system in a future time point, given the information of several previous states.

Also, a Linear Discriminat Analysis [44] was performed in the dataset, using the month of the year as the output discriminant value. A clear cluster structure can be obtained from this analysis, classifying correctly a 95.1 % of the cases, so it seems interesting to split data used in experiments for training and testing by months. The scatterplot of this initial analysis can be found on Figure 6.

Two different batches of data were selected for performing the experiments. In the first batch, the complete set of readings were used to train different regression models. In the second batch, only the readings corresponding to time instants where the pump was not turned off in a steady state were considered. To do this, samples in which the temperature difference between sensors S28 and sensor S29 (considered as the output and input sensors respectively) are equals or lower than 1 degree Celsius, were filtered out. As a result, in the second batch of data, dataset was reduced to 6.735 samples.

The aim of this approach is to assess whether using all data is necessary to build an accurate prediction system or fewer is enough. This would increase computing efficiency by reducing storage and computational needs.

The objective considered is to be able to predict the temperature registered on sensor S28, given different subsets of data selected from the dataset. Other aim of the study is to determine if a system that predicts accurately future behaviors of the heat exchanger can be developed by using a lower number of sensors on it. Since all the sensors are distributed on a connected system, there is a strong correlation between them. Therefore, there are few dimensions that are really necessary to capture the system's behavior, since the rest are related to it. In our experiments only measures obtained from S28 and S401 (ground temperature) have been used.

In order to compare models for regression in our case, we have selected several types of models: statistical models such as Decision Tree or Ridge Regression were used in a first stage, also including a more accurate model such as the Multi-Layer Perceptron (MLP). The results of these are compared with more advanced conexionist models on the family of the Time Dependent Neural Networks (TDNN), which have been designed for this type of task in particular. Several other statistical models (K-Nearest Neighbors, Support Vector Machines) have been tested, but are not included in the results shown as results were worse than those. Parameters have been adjusted by a random search method.

5. Experiment Results

5.1. Error Measures

This section briefly introduces the concepts of Mean Square Error (MSE), Mean Absolute Error (MAE), Median Absolute Error (MDAE) and Coefficient of Determination (R^2). These parameters are used as quality measure of the methods performance. We can find several examples in the literature that use these errors to asses the performance of temperature and forecast prediction and analysis, such as [45, 46, 47]. For a deep revision into forecasting errors we recommend [48].

Mean Square Error :

Supposing $(\hat{X}_i)$ be the vector denoting values of n number of predictions, and X_i be a vector representing n number of true values, the Mean Square Error is defined as: $MSE = \frac{1}{n}\sum_{i=1}^{n}(\hat{X}_i - X_i)^2$

Mean Absolute Error :

Model	Parameters
Ridge Regression	Regularization strength (α): 975
ARIMA	autoregressive (p): 0 differencing (d): 0 moving-average (q): 1
Decision Tree	Max depth: 15 Min samples Leaf: 45 Min samples Split: 40

(a) Statistical Regressors training parameters used in the experiments

Model	Parameters
Multi-Layer Perceptron	Activation: rectified linear unit function Num hidden layers: 1 Num neurons: 10
NAR	Num Delays: 6 Num hidden Layers: 1 Num neurons: 10
NARX	Num Delays: 6 Num hidden Layers: 1 Num neurons: 10
NIO	Num Delays: 6 Num hidden Layers: 1 Num neurons: 10

(b) ANNs training parameters used in the experiments

Table 1: Experimental Models Parameters

The definition is similar to MSE, but in this case, the direction or sign of the error is not taken into account.

With the same notation, that in MSE we can define $MAE = \frac{1}{n}\sum_{i=1}^{n}|\hat{X}_i - X_i|$

Median Absolute Error :

It consists of substituting the mean in MAE by the median: $MDAE = median\sum_{i=1}^{n}|\hat{X}_i - X_i|$

Coefficient of Determination :

R^2 is used to analyse how differences in one variable can be explained by a difference in a second variable. In other words, is the proportion of the variance in the dependent variable that is predictable from the independent variables. $R^2 = 1 - \frac{\sum_{i=1}^{n}(\hat{X}_i - \bar{X})^2}{\sum_{i=1}^{n}(X_i - \bar{X})^2}$

5.2. Results

As a mean of comparison, a test has been completed using the same readings of the S28 sensor to predict the value of the S28 in 3 different time horizons in the future. That is assuming that, in 1 hour, 3 hours or 6 hours time, the temperature will be the same as in the reference time instant. The results are presented in terms of the well-known error measures calculated for regression problems: Mean Absolute Error (MAE), Mean Square Error (MSE), Median Absolute Error (MDAE) and Coefficient of Determination (R^2). These error results are included in Table 2. As expected, results are not very satisfactory and can be improved greatly with the use of regression models.

In the experiments, different regression models are compared when modeling the future behavior of the system taking into account previous states of the same system. For the statistical and MLP models, given an instant in time, the current state of the ground temperature (S401), and the previous six measurements of sensor S28 are considered as inputs. The outputs represent the predicted current value of S28, the predicted next value of S28 (corresponding to the following 10 minutes) and the predicted values of S28 in one, three and six hours. The NAR model has only two inputs and one output. One input represents the current state of S28 and the other represents the number of step delays taken into account to predict the output, which is the value of S28 after n minutes. Since TDNN techniques do not

	All Data				Only when pump is working			
Time Horiz.	MAE	MSE	MDAE	R^2	MAE	MSE	MDAE	R^2
1 h	1.05	4.29	0.56	0.82	1.55	3.45	1.36	-0.15
3 h	1.87	10.06	1.23	0.41	3.15	12.63	2.99	-4.27
6 h	2.45	14.72	1.58	0.11	4.37	24.82	3.91	-9.90

Table 2: Regression errors obtained when using the same S28 time series data to try to predict the value of the series in different time horizons

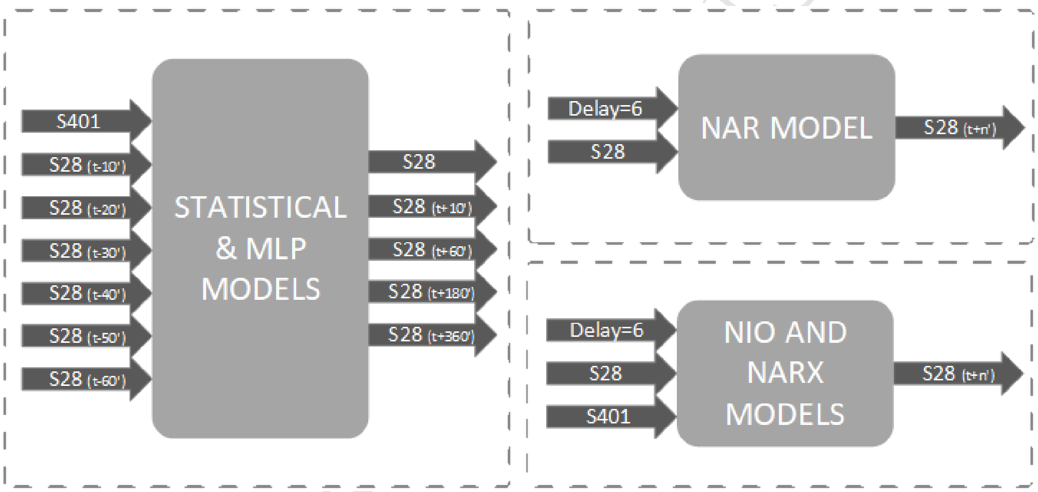

Figure 7: Model configuration depending on the technique applied

allow predicting more than one output, a different model is obtained for each output prediction (one, three and six hours in advance). In addition to the NAR inputs, NIO and NARX models use an external input corresponding to sensor S401. Figure 7 summarizes the configuration of each model.

The dataset was in all experiments divided into 12 folds of samples contiguous in time. To compare the effect of the amount of data used to train a model in the final regression, two sets of experiments were considered. In one set of experiments, the model is trained only with a given fold and tested with the next one in time, and in the other set, the model was trained with all data available until a given point in time and tested with the following fold in time. This means that, both when training with all data samples or when doing so with samples where the heat pump was not turned off in a steady state, the results shown are the mean of a 12-fold validation of the model in the whole year.

Tests have been performed training the models with different time horizons; that is, trying to predict the value in different time instants in the future. Experiments have been completed training the models to predict the temperature value of the system in 1 hour time, in 3 hours time and in 6 hours time, given the readings of the previous hour as an input to all models.

5.3. Training with all data

The results shown in Table 3 have been calculated over all the data available. Two different training variations have been tested: the first one consisted of using only the previous month to predict the next one, while the second one consisted of training with all data available up to a certain point to predict the measures for the next month. As expected, the NIO model values are clearly worse than the rest of the models and have not been included in the tables, for space reasons. They have been nevertheless included in Figure 8 for comparison purposes.

As an immediate conclusion, it is clear that the TDNN based models outperform in all cases the rest of the standard regression ones. As a general case, NAR model shows the best performance in almost all cases. That means that the inclusion of the ground temperature, as an external data source, in this case does not include any clearly valuable information to the series prediction, since the main difference between NAR and NARX is the inclusion of this external information. That seems to point to the idea that the performance of the system depends more on the previous states of the system than the external conditions, reinforcing the idea of the importance of a good system modeling.

What is even more interesting is that while the performance of the other models degrades when the distance in time to predict increases, TDNNs behave in a different way: NAR models maintain slightly the same performance in the three cases and NARX models even improve in a clear way when the time horizon becomes more distant.

It is interesting to note in the case of generalist regressors, when the algorithm is trained with the accumulated of all data preceding the analyzed set, the resulting error measures are very similar or even slightly worse than when the models are trained only with the data included in the previous month. This is expected, as the inclusion of training samples from very distant points

		Trained by month				Trained with the accumulated			
Time Horiz.	Model	MAE	MSE	MDAE	R^2	MAE	MSE	MDAE	R^2
1 h	Ridge	0.61	1.26	0.23	0.96	0.70	1.49	0.38	0.94
	ARIMA	1.00	3.83	0.37	0.86	1.36	6.75	0.56	0.76
	DecTree	0.95	2.40	0.36	0.91	0.97	2.74	0.32	0.90
	MLP	0.70	1.57	0.25	0.94	0.87	1.98	0.41	0.93
	NAR	**0.18**	**0.25**	**0.06**	**0.99**	**0.23**	**0.30**	**0.11**	**0.99**
	NARX	1.60	6.34	0.78	0.77	**0.36**	**0.36**	**0.26**	**0.99**
3 h	Ridge	1.03	3.01	0.49	0.89	0.96	2.57	0.52	0.91
	ARIMA	1.86	8.60	0.83	0.66	2.25	8.66	1.60	0.66
	DecTree	1.91	10.62	0.81	0.62	1.73	9.44	0.59	0.66
	MLP	1.18	3.23	0.61	0.88	1.25	3.16	0.77	0.89
	NAR	**0.20**	**0.27**	**0.06**	**0.99**	**0.22**	**0.26**	**0.10**	**0.99**
	NARX	1.02	3.22	0.43	0.88	**0.23**	**0.30**	**0.15**	**0.99**
6 h	Ridge	1	5.86	0.68	0.79	1.52	5.86	0.87	0.79
	ARIMA	17.67	14.34	18.12	0.49	3.20	15.05	2.60	0.47
	DecTree	2.75	17.91	1.31	0.36	2.32	14.49	0.95	0.48
	MLP	2.11	10.40	1.81	0.63	1.91	9.13	1.01	0.67
	NAR	**0.18**	**0.29**	**0.06**	**0.99**	**0.28**	**0.53**	**0.09**	**0.98**
	NARX	0.74	1.81	0.30	0.93	0.52	0.63	0.30	0.98

Table 3: Error measures obtained for the studied regression models. Data represents the mean measure obtained for the 12 cross-validation folds, measured on the complete dataset. Data samples gathered both when the exchanger is functioning and not functioning are used for the error calculation.

in time along a complete year will probably lead towards overfitted models. On the other hand, while this is true also for the NAR model, this situation is reversed in the case of the NARX: using all data available helps this model to consistently obtain lower errors. This is easily appreciated in Figure 8.

In this figure it is also noticeable some of the features of the problem and the results obtained: i.e. in the readings of the summer months (June, July, August), the exchanger is functioning very rarely, so the error in the prediction decreases clearly in all models. When using the accumulation of data to train the models, error usually decreases in the TDNN models, while it remains almost the same for the rest of the models (which is higher than the TDNN in both cases). This would suggest that a straightforward direction to continue the study would be the use of data from different years to study the effects of its inclusion in the training sets. As mentioned before, the NIO models, which does not include in its architecture a feedback loop, is the worst performing of the models.

This can be observed also when representing the values obtained from each model along with the real value to predict, as are represented in Figure 9 and Figure 10.

Again, by inspecting Figure 9 and Figure 10, it seems that the inclusion of the external variables, taking into account results only in a too close period of time has the effect of overfitting in the NARX and in a lower degree, the NAR. The use of data from the previous month predictions seems to stay in a lower range, probably because none of the samples went above that temperature. When considering data from several months before, the network training enables it to generalize better. The opposite results happens for the Ridge model: even when the regression is not as good in neither of the comparisons, when using only data from one month seems to cause less overfitting (the measures are a bit closer to the real value in this case). Less advanced models seem to profit from a lower amount of data from closer instants in time.

When the pump is not in operation for a time, the temperature of the sensor S28 remains nearly constant. Since the complete dataset includes a majority of readings in which the pump of the heat exchanger is in a repose state, this situation can hinder the real error results we wanted to measure: the prediction of the conditions of the heat pump when it is working. Given that the temperature on S28 does not vary when the pump is off in a steady state, a regression model would not be necessary in this case. After removing the data when the pump is off in a steady state, the second subset of

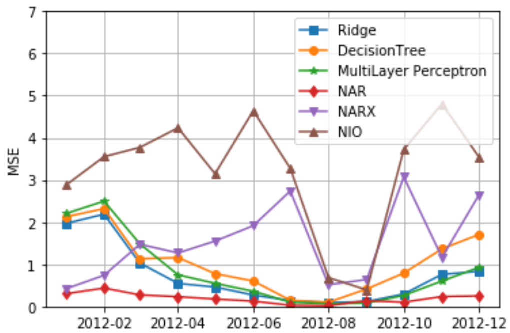

(a) MSE for 1 hour time horizon, when models are trained only with data from the previous month

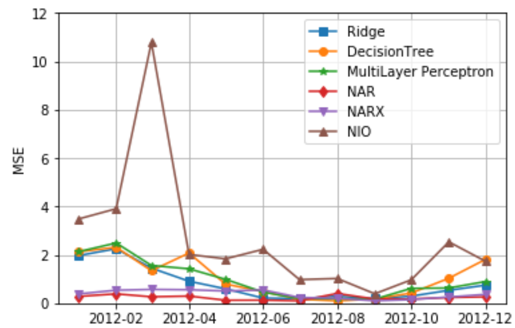

(b) MSE for 1 hour time horizon, when models are trained with all data available up to each month

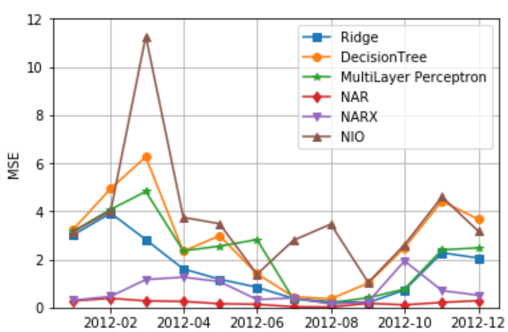

(c) MSE for 6 hour time horizon, when models are trained only with data from the previous month

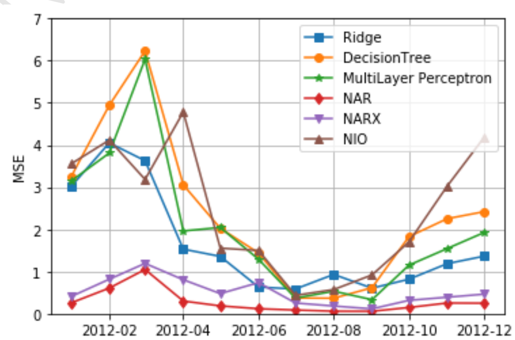

(d) MSE for 6 hour time horizon, when models are trained with all data available up to each month

Figure 8: MSE obtained for each of the compared models in each month of the year

Figure 9: Example of the regression values obtained for each of the models, all of them calculated for a time horizon of 1 hour. The first week of March 2012 is shown as an illustrative example. Results when models are trained with data obtained from all previous time instants (January-February 2012).

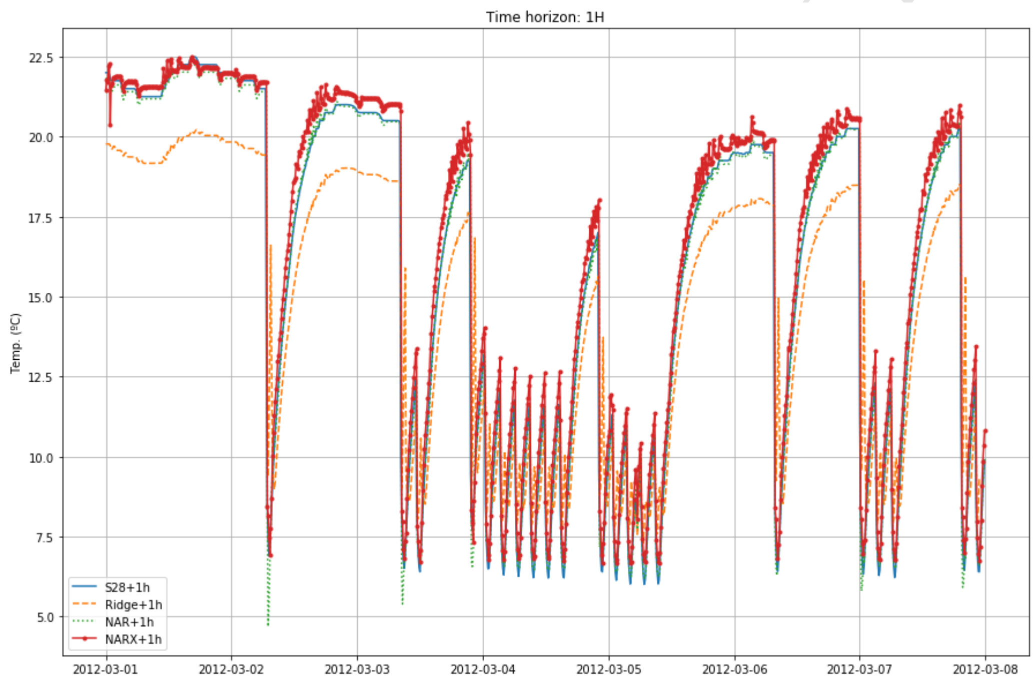

Figure 10: Example of the regression values obtained for each of the models, all of them calculated for a time horizon of 1 hour. The first week of March 2012 is shown as an illustrative example. Results when models are trained with data obtained only from the previous month (February 2012).

data described in Section 4 is used to calculate error measures. In this re-calculations of errors, the predictions used are the same as in Table 3; with the only difference that the subset of the predictions made when the pump is off in a steady state are filtered out.

The results obtained re-calculating errors over only the working samples are shown in Table 4.

Analyzing Table 4 is easy to observe that, as expected, errors are clearly higher for all models, as we are now discarding samples where the pump was not functioning in a steady state and therefore the prediction was almost identical to the input. Nevertheless, it is interesting to note that all the remarks applied to the errors obtained from the whole dataset are present in this results too: TDNN models are the best performing ones and the difference in the time horizon only has a slight influence in the results.

5.4. Training only with data when working

Observing the results of section 5.3, specially those of Table 4, in which calculating the error only in the time instants when there was activity in the exchanger lead to higher error, one could wonder if this is an overfitting effect caused by training with data that could be interpreted as noise, since it conceals the data samples which are more interesting to predict. To check if that is the case, the last experiment consisted of training again the models with the same schema as the initial experiments (12 fold cross-validation and including only one month or the accumulated of the year), but including in each fold only the samples where the pump is not turned off in a steady state.

As expected, the use of a reduced dataset highly impacts the final results. This suggests that models would need to retrieve consistently equally time-spaced measurements from the data. Apart from the fact that depending on the months, the exchanger is active along longer periods of time (and therefore includes more data samples), the preservation of the temporal component of the data evenly spaced is determinant for the results. The fact that the readings of 1 hour are used as a complete input to predict a given time instant, should be the reason. The models can detect if the pump has begun to work in that period of time and adapt their prediction accordingly. In case of selecting just the working cases, that information is lost, since the model cannot identify if the functioning has begun or finished in given time instants before.

The results obtained when models with this subset are shown in Table 5: As expected, all results include a clearly higher error than when the

		Trained by month				Trained with the accumulated			
Time Horiz.	Model	MAE	MSE	MDAE	R^2	MAE	MSE	MDAE	R^2
1 h	Ridge	1.41	3.62	1.09	0.67	1.69	4.72	1.31	0.57
	ARIMA	3.97	24.21	3.22	0.17	3.84	22.17	3.21	0.17
	DecTree	2.00	6.30	1.70	0.43	1.93	5.90	1.48	0.46
	MLP	1.43	3.80	1.06	0.65	1.92	5.61	1.66	0.49
	NAR	**0.59**	**1.63**	**0.18**	**0.85**	**0.60**	**1.66**	**0.21**	**0.85**
	NARX	2.13	11.17	0.94	-0.02	**0.73**	**1.68**	**0.40**	**0.85**
3 h	Ridge	2.12	6.45	2.02	0.413	1.56	3.73	1.48	0.66
	ARIMA	4.52	30.03	3.78	0.18	4.13	25.66	3.46	0.06
	DecTree	3.26	15.26	3.09	-0.39	2.60	9.69	2.41	0.12
	MLP	2.12	7.13	1.76	0.35	1.77	4.67	1.70	0.57
	NAR	**0.59**	**1.55**	**0.23**	**0.86**	**0.62**	**1.62**	**0.25**	**0.85**
	NARX	1.2	3.34	0.79	0.69	**0.69**	**1.59**	**0.37**	**0.85**
6 h	Ridge	2.72	10.05	2.77	0.08	2.44	8.17	2.45	0.25
	ARIMA	3.98	22.62	3.56	-1.06	3.40	15.77	3.35	-0.43
	DecTree	14.77	35.50	14.74	0.14	4.29	26.54	3.86	0.13
	MLP	3.18	14.85	2.90	-0.35	2.94	11.78	2.85	0.07
	NAR	**0.63**	**1.78**	**0.23**	**0.84**	**0.56**	**1.51**	**0.19**	**0.86**
	NARX	1.06	2.85	0.63	0.74	0.79	1.78	0.42	0.84

Table 4: Error measures obtained for the studied regression models. Data represents the mean measure obtained for the 12 cross-validation folds, measured on the complete dataset. Only samples of dataset where the heat pump is working are used for the error calculation.

		Trained by month				Trained with the accumulated			
Time Horiz.	Model	MAE	MSE	MDAE	R^2	MAE	MSE	MDAE	R^2
1 h	Ridge	1.72	4.45	1.52	0.58	1.79	4.92	1.61	0.54
	ARIMA	-	-	-	-	-	-	-	-
	DecTree	1.81	4.77	1.70	0.55	1.86	5.50	1.68	0.48
	MLP	1.96	5.98	1.71	0.44	1.94	6.07	1.68	0.43
	NAR	2.29	10.47	1.67	0.02	2.16	9.09	1.53	0.14
	NARX	2.89	13.42	2.32	-0.26	2.51	14.25	1.86	-0.33

Table 5: Error measures obtained for the studied regression models. Data represents the mean measure obtained for the 12 cross-validation folds, measured only on samples of the dataset where the heat pump is working, both for training and for testing.

models are trained with the whole dataset, even if we are only comparing data samples when the pump is not stopped (as shown in Table 4). Since the errors on time horizons 3 hour and 6 hours are equally higher than those in the previous experiment, they have been left out of the table. The ARIMA model could not be calculated with this configuration of the dataset, since it needs evenly spaced in time data to be trained.

6. Conclusions and Future Work

The contribution presents a heat exchanger designed to help regulate the temperature of a bio-climatic installation. The research presented focuses its effort in proving that the behavior exhibited by this type of installation can be accurately modeled for later purposes, such as energy consumption expected in each of this bio-climatic homes to be able to achieve electrical smart grid applications.

As result of the analysis, one of the first conclusions is that the modeling of the system, can be achieved using very few of the sensors readings (two would suffice), as long as they are logging the measurements with a reasonable enough frequency: a 10 minutes frequency is used in our experiments. It is advisable to collect data without regarding the functioning mode of the installation, since the information captured in the transitions from one state to the other seem to be particularly important for the time series regression in this application.

Several modeling experiments have been performed, obtaining as a result an average prediction error of less than 1 degree Celsius as a mean along a complete year. The systems perform well both in the cases of a functioning and no functioning pump, being this transparent for the user: the system does not need this information to adapt its behavior.

The best performing models have been Time Dependent Neural Networks (TDNN), as they are designed precisely to capture and predict features attending to their variations along periods of time, to be able to predict future states by analyzing differences between previous states of the data.

Interesting directions to continue the work could include performing anomaly detection analysis in the functioning of the installations using the sensors, that would enable to prevent failures before they happen or correct undesirable performances in the system on the fly. Using data inputs form other related sensors in the building and even using external sources of information, such as meteorological data in order to combine data for more accurate predictions would be another clear direction. This could lead to test the regression capabilities of directly calculating the energy consumption of the bio-climatic home given enough information collected from different systems in previous time periods. This problem will be tackled in two different ways, both by trying techniques for information fusion previous to the training of the regression models and by training ensembles of regressors that can combine their outputs to improve the accuracy of the predictions or enhance them with additional information. Finally, the use of advanced prediction models involving more complex architectures, such as the Long-Short Term Memory (LSTM) Recurrent Neural Networks, which represents an evolution on the TDNN models; or other deep learning paradigms will be considered.

Acknowledgments

We would like to thank the 'Instituto Enerxético de Galicia' (INEGA) and 'Parque eólico Experimental de Sotavento' (Sotavento Foundation) for their technical support on this work.

References

[1] E. C. (EC), Europe 2020: a strategy for smart, sustainable and inclusive growth, Working paper {COM (2010) 2020} (2010).

[2] D. Porter, Comprehensive Renewable Energy, Elsevier, 2012.

[3] S. Jacobsson, V. Lauber, The politics and policy of energy system transformation—explaining the german diffusion of renewable energy technology, Energy policy 34 (2006) 256–276.

[4] M. Kaltschmitt, W. Streicher, A. Wiese, Renewable Energy, Springer Berlin Heidelberg, 2007.

[5] T. Jenssen, Glances at Renewable and Sustainable Energy, Springer London, 2013.

[6] O. Ozgener, L. Ozgener, Modeling of driveway as a solar collector for improving efficiency of solar assisted geothermal heat pump system: a case study, Renewable and Sustainable Energy Reviews 46 (2015) 210 – 217.

[7] M. H. Dickson, M. Fanelli, Geothermal energy: utilization and technology, Routledge, 2013.

[8] L. Ozgener, O. Ozgener, Monitoring of energy exergy efficiencies and exergoeconomic parameters of geothermal district heating systems (gdhss), Applied Energy 86 (2009) 1704 – 1711.

[9] L. Ozgener, A review on the experimental and analytical analysis of earth to air heat exchanger (EAHE) systems in turkey, Renewable and Sustainable Energy Reviews 15 (2011) 4483–4490.

[10] S. Kakaç, H. Liu, A. Pramuanjaroenkij, Heat Exchangers: Selection, Rating, and Thermal Design, Second Edition, Designing for heat transfer, Taylor & Francis, 2002.

[11] H. Sauer, R. Howell, Heat Pump Systems, Krieger Publishing Company, 1991.

[12] G. Florides, S. Kalogirou, Ground heat exchangers—a review of systems, models and applications, Renewable Energy 32 (2007) 2461 – 2478.

[13] A. Rezaei, E. Kolahdouz, G. Dargush, A. Weber, Ground source heat pump pipe performance with tire derived aggregate, International Journal of Heat and Mass Transfer 55 (2012) 2844–2853.

[14] O. Ozgener, L. Ozgener, D. Y. Goswami, Experimental prediction of total thermal resistance of a closed loop eahe for greenhouse cooling system, International Communications in Heat and Mass Transfer 38 (2011) 711 – 716.

[15] G. E. Box, G. M. Jenkins, G. C. Reinsel, G. M. Ljung, Time series analysis: forecasting and control, 2015.

[16] R. Burtiev, F. Greenwell, V. Kolivenko, Time series analysis of wind speed and temperature in Tiraspol, Moldova, volume 12, 2013.

[17] B. Iqelan, Time Series Modeling of Monthly Temperature Data of Jerusalem/Palestine, volume 31, 2015.

[18] A. HOERL, R. KENNARD, RIDGE REGRESSION - APPLICATIONS TO NONORTHOGONAL PROBLEMS, TECHNOMETRICS 12 (1970) 69–&.

[19] M. Pena, H. van den Dool, Consolidation of Multimodel Forecasts by Ridge Regression: Application to Pacific Sea Surface Temperature, JOURNAL OF CLIMATE 21 (2008) 6521–6538.

[20] H. Sun, H. Wang, The driving factors of the increase of the building energy consumption based on ridge regression, Urban Develop 5 (2013).

[21] F. Pedregosa, G. Varoquaux, A. Gramfort, V. Michel, B. Thirion, O. Grisel, M. Blondel, P. Prettenhofer, R. Weiss, V. Dubourg, J. Vanderplas, A. Passos, D. Cournapeau, M. Brucher, M. Perrot, E. Duchesnay, Scikit-learn: Machine learning in Python, Journal of Machine Learning Research 12 (2011) 2825–2830.

[22] C. J. Stone, Classification and regression trees., Wadsworth International Group 8 (1984) 452–456.

[23] E. G. Petre, A decision tree for weather prediction., Bulletin of PG University of Ploieşti, Series Mathematics, Informatics, Physics 61 (2009) 53–58.

[24] G. K. F. Tso, K. K. W. Yau, Predicting electricity energy consumption: A comparison of regression analysis, decision tree and neural networks, ENERGY 32 (2007) 1761–1768.

[25] H. Yu, Y. Chen, S. G. Hassan, D. Li, Prediction of the temperature in a Chinese solar greenhouse based on LSSVM optimized by improved PSO, COMPUTERS AND ELECTRONICS IN AGRICULTURE 122 (2016) 94–102.

[26] W. Y. Loh, Classification and regression trees, iley Interdisciplinary Reviews: Data Mining and Knowledge Discovery 1 (2011) 14–23.

[27] D. E. Rumelhart, G. E. Hinton, R. J. Williams, Learning representations by back-propagating errors, Nature 323 (1986).

[28] M. Hayati, Z. Mohebi, Application of Artificial Neural Networks for Temperature Forecasting, in: Ardil, C (Ed.), PROCEEDINGS OF WORLD ACADEMY OF SCIENCE, ENGINEERING AND TECHNOLOGY, VOL 22, volume 22 of *Proceedings of World Academy of Science Engineering and Technology*, WORLD ACAD SCI, ENG & TECH-WASET, PO BOX 125, CANAKKALE, 17100, TURKEY, 2007, pp. 275–279. Conference of the World-Academy-of-Science-Engineering-and-Technology, Prague, CZECH REPUBLIC, JUL 27-29, 2007.

[29] S. Karatasou, M. Santamouris, V. Geros, Modeling and predicting building's energy use with artificial neural networks: Methods and results, ENERGY AND BUILDINGS 38 (2006) 949–958.

[30] P. H. Shaikh, N. B. M. Nor, P. Nallagownden, I. Elamvazuthi, T. Ibrahim, A review on optimized control systems for building energy and comfort management of smart sustainable buildings, RENEWABLE & SUSTAINABLE ENERGY REVIEWS 34 (2014) 409–429.

[31] J.-L. Casteleiro-Roca, E. Jove, J. M. Gonzalez-Cava, J. A. M. Pérez, J. L. Calvo-Rolle, F. B. Alvarez, Hybrid model for the ani index prediction using remifentanil drug and emg signal, Neural Computing and Applications (2018) 1–10.

[32] E. Jove, J. M. Gonzalez-Cava, J.-L. Casteleiro-Roca, J.-A. Méndez-Pérez, J. Antonio Reboso-Morales, F. Javier Pérez-Castelo, F. Javier de Cos Juez, J. Luis Calvo-Rolle, Modelling the hypnotic patient response in general anaesthesia using intelligent models, Logic Journal of the IGPL (2018).

[33] E. Jove, J. Antonio Lopez-Vazquez, M. Isabel Fernandez-Ibanez, J.-L. Casteleiro-Roca, J. Luis Calvo-Rolle, Hybrid intelligent system to predict the individual academic performance of engineering students, INTERNATIONAL JOURNAL OF ENGINEERING EDUCATION 34 (2018) 895–904.

[34] A. WAIBEL, T. HANAZAWA, G. HINTON, K. SHIKANO, K. LANG, PHONEME RECOGNITION USING TIME-DELAY NEURAL NETWORKS, IEEE TRANSACTIONS ON ACOUSTICS SPEECH AND SIGNAL PROCESSING 37 (1989) 328–339.

[35] A. Yona, T. Senjyu, A. Y. Saber, T. Funabashi, H. Sekine, C.-H. Kim, Application of neural network to one-day-ahead 24 hours generating power forecasting for photovoltaic system, in: 2007 INTERNATIONAL CONFERENCE ON INTELLIGENT SYSTEMS APPLICATIONS TO POWER SYSTEMS, VOLS 1 AND 2, IEEE; IEEE Power Engn Soc; Natl Sci Council; Minist Educ; Taiwan Power Co; Allis Elect Co Ltd; Hsiang Chen Elect Corp; ABB; Shingneng Power Co; Taiwan Cogenerat Corp; Siemens; Shihlin Elect & Engn Corp; Natl Sun Yat Sen Univ, IEEE, 345 E 47TH ST, NEW YORK, NY 10017 USA, 2007, pp. 423+. 14th International Conference on Intelligent System Applications to Power Systems (ISAP 2007), Kaohsiung, TAIWAN, NOV 04-08, 2007.

[36] M. Valipour, Optimization of neural networks for precipitation analysis in a humid region to detect drought and wet year alarms, METEOROLOGICAL APPLICATIONS 23 (2016) 91–100.

[37] P. Gonzalez, J. Zamarreno, Prediction of hourly energy consumption in buildings based on a feedback artificial neural network, ENERGY AND BUILDINGS 37 (2005) 595–601.

[38] L. G. Baca Ruiz, M. Pegalajar Cuellar, M. Delgado Calvo-Flores, M. D. C. Pegalajar Jimenez, An Application of Non-Linear Autoregressive Neural Networks to Predict Energy Consumption in Public Buildings, ENERGIES 9 (2016).

[39] I. The MathWorks, Matlab and statistics toolbox release 2017b, 2017. Natick, Massachusetts, United States.

[40] T. Lin, B. Horne, P. Tino, C. Giles, Learning long-term dependencies in NARX recurrent neural networks, IEEE TRANSACTIONS ON NEURAL NETWORKS 7 (1996) 1329–1338.

[41] M. Ramasamy, H. Zabiri, N. T. T. Ha, N. M. Ramli, Heat exchanger performance prediction modeling using NARX-type neural networks, in: Helmis, C and Celikyay, S (Ed.), LECTURE NOTES ON ENERGY AND ENVIRONMENT, Energy and Environmental Engineering Series, WSEAS, WORLD SCIENTIFIC AND ENGINEERING ACAD AND SOC, AG LOANNOU THEOLOGOU 17-23, 15773 ZOGRAPHOU, ATHENS, GREECE, 2007, pp. 202+. WSEAS International Conference on Renewable Energy Sources/Energy Planning, Energy Saving, Environmental Education/Waste Management, Water Pollution, Air Pollution, Indoor Climate, Arcachon, FRANCE, OCT 14-16, 2007.

[42] S. Wei, D. Zuo, J. Song, Improving prediction accuracy of river discharge time series using a Wavelet-NAR artificial neural network, JOURNAL OF HYDROINFORMATICS 14 (2012) 974–991.

[43] E. Cadenas, W. Rivera, R. Campos-Amezcua, C. Heard, Wind Speed Prediction Using a Univariate ARIMA Model and a Multivariate NARX Model, ENERGIES 9 (2016).

[44] G. J. McLachlan, Discriminant Analysis and Statistical Pattern Recognition, John Wiley & Sons, 2005.

[45] e. a. Sullivan, J., Observation error statistics for noaa-10 temperature and height retrievals., Monthly weather review 121 (1993) 25782578–2587.

[46] K. A. Emanuel, M. Živković Rothman, Development and evaluation of a convection scheme for use in climate models., Journal of the Atmospheric Sciences 56 (1999) 1766–1782.

[47] e. a. Juhana, H., Error characteristics of temperature forecast in finland for the period 1979–2011 in relation to various weather patterns., Meteorological Applications 23 (2016) 244–253.

[48] e. a. Shcherbakov, M. V., A survey of forecast error measures., World Applied Sciences Journal 24 (2013) 171–176.

Highlights of "Geothermal heat exchanger energy prediction based on time series and monitoring sensors optimization"

- The performance prediction of a geothermal heat exchanger can improve its efficiency.
- From real measurements, the system is modelled with intelligent techniques.
- The models predict the state of the installation up to 6 hours in advance.
- A strong correlation between different sensors is concluded.